

Analysis of the Look-Locker T_1 mapping sequence in dynamic contrast uptake studies: simulation and in vivo validation

Magnus Karlsson*, Bo Nordell

MR Research Center, Karolinska Institute and Department of Medical Radiation Physics, Karolinska Institute, Stockholm, Sweden

Received 14 June 2000; accepted 23 August 2000

Abstract

An alternative to the pulse sequences at present used in dynamic contrast uptake MRI is the dynamic LL-EPI T_1 mapping method. This method generates T_1 estimates in a few seconds, thereby allowing dynamic studies. A particular advantage of the LL-EPI technique is that it provides the opportunity to generate spatial and temporal information about the paramagnetic contrast agent concentration independently of the inflow rate. This paper illustrates, by computer simulations, the accuracy of the estimated $1/T_1$ value when using the LL-EPI technique in situations that are not supported by the model. The simulated situations not supported by the model are those in which the longitudinal and transversal relaxation rates change during the T_1 mapping. The most critical moment occurs during a bolus passage of contrast agent when the concentration gradient is large. The computer simulations of the LL-EPI T_1 mapping method in non-supported situations show that in normal perfused capillary tissue the error in the estimated $1/T_1$ value is within the absolute error of 0.1 s^{-1} in most simulated situations, although in a typical vessel the simulations do indicate that the stated absolute error tolerance of 0.5 s^{-1} is exceeded relatively easily. However, this transgression can be rectified by a non-bolus injection of the contrast agent media. © 2000 Elsevier Science Inc. All rights reserved.

Keywords: Dynamic MRI; LL-EPI; T_1 mapping

1. Introduction

Dynamic contrast uptake studies with magnetic resonance imaging (MRI) have recently emerged as a promising method for obtaining information about tumor vascularization [1]. Usually these studies are based on dynamic contrast-enhanced T_1 -weighted MRI data acquired by a gradient-echo (or spin-echo) pulse sequence [2–4]. A limitation of this technique is the difficulty in getting a proper input-function curve to monitor the contrast agent concentration of the blood. This is because the signal enhancement due to inflow dominates the signal enhancement due to T_1 relaxation shortening in large vessels with high flow perpendicular to the imaging plane. A possible method of reducing the inflow effect is to use a T_1 -weighted, magnetization-prepared fast gradient-echo sequence with a non-slice selective magnetization preparation [5,6].

An interesting alternative to these techniques is dynamic T_1 mapping. Normally, T_1 mapping is a time-consuming process, but by using a combination of the Look-Locker sequence [7] (LL) and echo-planar imaging [8] (EPI) a T_1 map can be generated in less than 3 seconds [9,10]. An advantage of the LL-EPI sequence is that the concentration of paramagnetic contrast agents, such as Gd-DTPA and gadodiamide, is proportional to the longitudinal relaxation rate [11–13] ($1/T_1$). A further advantage of the dynamic LL-EPI T_1 mapping method is its insensitivity to inflow effects [14], which gives the option of dynamically tracking the contrast agent concentration in a vessel.

Using the LL-EPI T_1 mapping method in dynamic uptake studies can, however, lead to pitfalls if the assumptions made in the theory [14] are exceeded. In this paper, one kind of transgression is illustrated, namely when the longitudinal and transversal relaxation rates change during the T_1 mapping. Bloch-equation computer simulations have been performed and an in vivo material has been studied and compared with the outcome of the simulations.

* Corresponding author. Tel.: +46-8-5177-6116; fax: +46-8-5177-6111.

E-mail address: magnus@mrc.ks.se (M. Karlsson).

2. Theory

The LL-EPI sequence for dynamic mapping of T_1 consists of a non-slice selective inversion pulse followed by multiple low flip-angle (α) slice selective excitation pulses to repeatedly sample the longitudinal magnetization during its recovery. The MRI signal is acquired as a single-shot gradient recalled EPI echo-train. On the assumption that partial volume effects are small, and there exists a fast exchange of water within the voxel, the acquired signal during the mapping can be described, as previously shown [14], by the equation:

$$S(t) = |A - B \cdot e^{-t(1/T_1 - \chi \ln(\cos\alpha)/\tau)}| \quad (1)$$

where t is the time after the inversion, τ is the time between the alpha pulses and α is the flip-angle of the alpha pulses. A and B are constants depending on the gain of the receiver circuit, the longitudinal magnetization at thermal equilibrium and the transversal relaxation rate ($1/T_2^*$). χ is a compensation constant between 0 and 1 to correct for the fact that spins flowing into the slice during the mapping are not exposed to all of the alpha pulses. Without any inflow χ equals 1, but if, on the other hand, all the spins are replaced between two alpha pulses χ will equal 0.

An effective relaxation rate $1/T_{1,eff}$ can be defined, which will depend on the previously defined α , τ and χ :

$$\frac{1}{T_{1,eff}} = \frac{1}{T_1} - \frac{\chi \cdot \ln(\cos\alpha)}{\tau} \quad (2)$$

After an MRI data acquisition, a $T_{1,eff}$ map can be calculated by applying a three-parameter (A , B , $T_{1,eff}$) Levenberg-Marquardt [15] non-linear least-squares fit to Eq. (1) on a voxel-by-voxel basis.

In a previous paper [14] it was shown that the change in the longitudinal relaxation rate could be calculated using the following equation:

$$\Delta \frac{1}{T_1(t)} = \frac{1}{T_{1,eff}(t)} - \frac{1}{T_{1,eff}(0)} \quad (3)$$

where t ($t > 0$) is an arbitrary time after the injection of contrast agent. Because the change in the longitudinal relaxation rate is proportional to the contrast agent concentration, dynamic $T_{1,eff}$ mapping with the LL-EPI technique generates temporal information about the contrast agent concentration in a specific voxel or volume of interest (VOI).

However, this dynamic T_1 mapping method is only valid if the following two criteria are fulfilled. First, the longitudinal and transversal relaxation rates must be constant during each T_1 mapping. Second, the inflow rate must be constant during the whole scan, i.e., during all the T_1 mappings. It is not likely that the inflow would change very much during the scan (minutes), so we have focused on the first criterion. This criterion is not fulfilled if the inflow in a VOI is high and the contrast agent concentration changes

rapidly in the blood, as for example during a bolus passage of contrast agent. If the first criterion presented above is fulfilled, the longitudinal magnetization will recover mono-exponentially during the LL-EPI T_1 mapping, according to Eq. (1). This, however, is not the case when the longitudinal and transversal relaxation rates vary during the T_1 mapping.

Fig. 1 shows signal behavior during simulated T_1 mappings with the LL-EPI method under different conditions. Fig. 1A–B illustrates simulated situations when the model is valid and Fig. 1C–D situations when the model conditions are exceeded. In Fig. 1C–D, the data stand out from mono-exponential recovery due to an increase of contrast concentration during the mapping. The parameters used in the simulations are given in the figure legend. Because Eq. (1) is simple and robust, we have chosen not to modify it, but instead to study its ability to calculate a proper $1/T_1$ or $1/T_{1,eff}$ in the non-supported conditions defined above. We have chosen to do this since the introduction of more variables into Eq. (1) to achieve better modeling would increase the degrees of freedom and create instability.

3. Methods

3.1. Simulations

We have made Bloch-equation computer simulations to simulate how the estimated $1/T_1$ and $1/T_{1,eff}$ values are affected if T_1 mapping is performed under non-supported conditions. In these simulations, two different inflow quantities were used, 10 voxel volumes per second as in a typical large vessel (sagittal sinus) voxel and 0.01 voxel volumes per second as in a normal perfused (60 mL/dL/min) micro-vessel (capillary) tissue or tumor voxel. The simulated voxel with high flow will hereafter be referred to as the vessel voxel and the simulated normal perfused micro-vessel voxel will be referred to as the tissue voxel. In the vessel voxel the blood volume of the voxel was assumed to be 1, meaning that the entire voxel is covered by the vessel. In the normal perfused tissue, the extraction fraction of the contrast agent was assumed to be 1, meaning that all the contrast agent that enters the voxel is absorbed. This assumption is the worst case scenario. Normally, for example, the extraction rate is about two to four times lower, resulting in only a fraction of the in-flowing contrast agent being absorbed in the voxel. To limit the number of cases, only four different scan parameter set-ups (A–D) of the LL-EPI sequence were studied, as shown in Table 1.

In the computer simulations, the Bloch equations were used to follow the magnitude of the longitudinal magnetization vector during the T_1 mapping time. The transversal decay was also taken into consideration. In the simulations, perfect slice profiles of the excitation pulses were assumed. Moreover, completely spoiled transversal magnetization was assumed before each excitation pulse. In the simulations, a T_1 relaxivity of $4.3 \text{ mM}^{-1} \text{ s}^{-1}$ and a T_2^* relaxivity

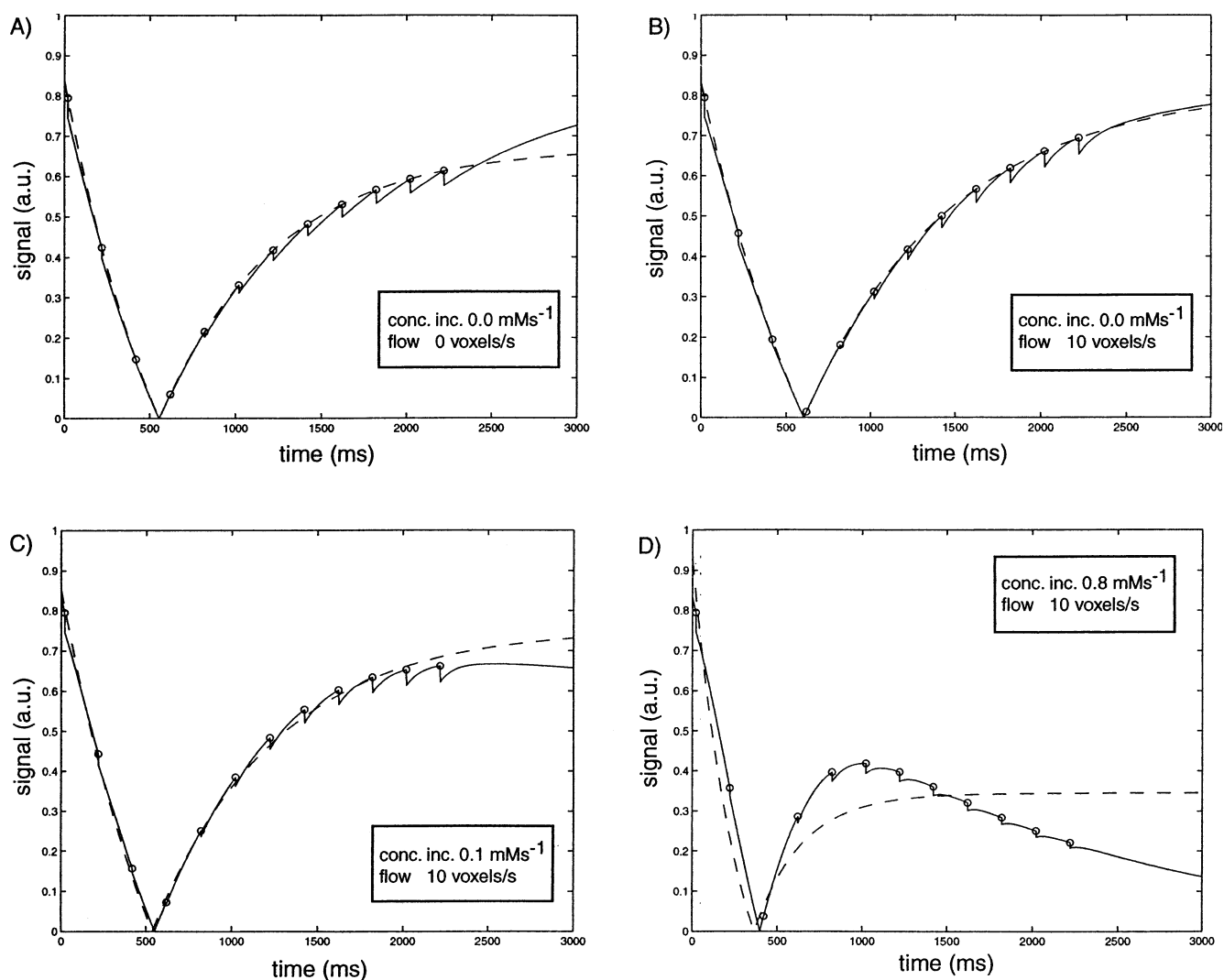


Fig. 1. Simulations of the MRI signal during LL-EPI T_1 mappings. The signal is calculated as the absolute value of the longitudinal magnetization compensated for transversal (T_2^*) decay. The circles indicate the theoretical measuring points and the dashed line the least-squares fits of the theoretical measuring points. In A–D the scan parameter set-up A (Table 1) is used and a starting contrast concentration of 0.1 mM is assumed. A, no inflow was assumed. B, a flow of 10 voxel volumes per second was assumed. C, the contrast concentration of the in-flowing tissue was assumed to increase linearly by 0.1 mM s^{-1} with an inflow as in B. D, as C, but with a contrast concentration increase of 0.8 mM s^{-1} .

of 53 $mM^{-1} s^{-1}$ were used. These values are based on previous reports [14,16] and our own measurements (not presented) on Gd-DTPA and gadodiamide at 1.5 T, and on the assumption that the T_2^* relaxivity is ten times larger than

Table 1
The four different LL-EPI parameter set-ups used in the simulations

Set-up	τ_0 (ms)	τ (ms)	TE (ms)	α ($^\circ$)	n
A	20	200	15	20	12
B	20	100	15	20	12
C	20	200	15	40	12
D	20	200	45	20	12

τ_0 is the time between the inversion pulse and the first alpha pulse, τ is the time between each two alpha pulses, TE is the echo time, α is the flip-angle of the alpha pulses, n is the number of alpha pulses.

the T_2 relaxivity. Because it is difficult to estimate the regional in vivo T_2^* relaxivity, we have chosen two similar set-ups (A and D), but with different echo times to attain different T_2^* dependencies.

In the simulations, we have focused on four T_1/T_2^* pairs, namely 1400/140, 873/81, 349/30 and 199 ms/17 ms, which are representative relaxation values for many human tissues and tumor types. These relaxation values can also be seen as the relaxation values in blood at the contrast agent concentrations 0, 0.1, 0.5 and 1.0 mM, if the named T_1 and T_2^* relaxivities are used. The estimated $1/T_1$ is calculated by applying a non-linear least-squares fit to Eq. (1) and then transforming $1/T_{1,eff}$ to $1/T_1$ using Eq. (2). The ideal $1/T_1$ value in the simulations is calculated as the weighted mean of $1/T_1$ during the time of the mapping. This value will hereafter be referred to as $1/T_{1,ideal}$ and the difference be-

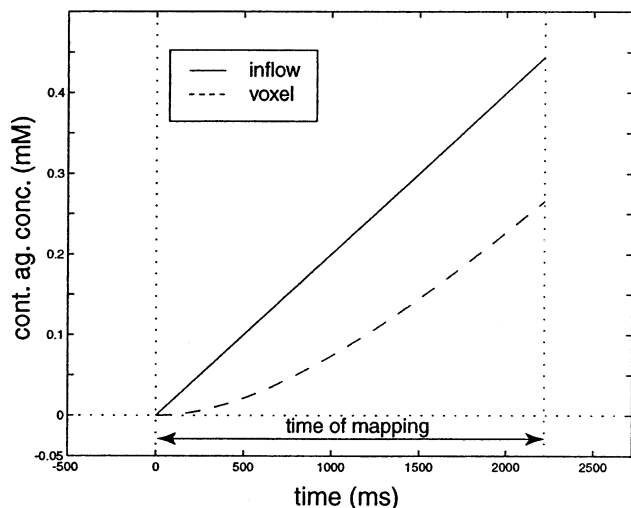


Fig. 2. This figure shows schematically how the contrast agent concentration of the in-flowing tissue (solid line) changes during the T_1 mapping and its effect on the contrast agent concentration in the voxel (dashed line). In the plot it is assumed that the inflow rate is 1 voxel volume per second.

tween the estimated $1/T_1$ and $1/T_{1,\text{ideal}}$ will be referred to as $1/T_{1,\text{error}}$ ($= 1/T_1 - 1/T_{1,\text{ideal}}$).

The main idea of this paper was to simulate the T_1 mapping situation in which the longitudinal and transversal relaxation rates change during the mapping, e.g. as after an injection of contrast agent. We have therefore let the contrast agent concentration of the in-flowing tissue increase or decrease linearly with time during the mapping.

At the beginning of a simulated mapping, the contrast concentration, and the relaxation rates are assumed to be the same in the voxel and in the in-flowing tissue. The four established T_1 and T_2^* values presented above were used as starting values and the contrast concentration in the voxel was allowed to change during the mapping as a result of the changing contrast concentration of the in-flowing tissue. See Figure 2. In the simulations, the contrast concentration of the in-flowing tissue was allowed to increase or decrease up to 1 mM s^{-1} . This value was chosen after analyzing our in vivo contrast uptake curves (not presented) which are similar to the uptake curve presented in a previous paper [14].

In vivo uptake curves [14] of a paramagnetic contrast agent show that $\Delta 1/T_1$ in blood can exceed 10 s^{-1} and in tumor tissue 2 s^{-1} . Based on these data we have chosen an absolute error tolerance of 0.5 s^{-1} for $1/T_{1,\text{err}}$ in the vessel voxel and 0.1 s^{-1} in the tissue voxel.

3.2. In vivo

As a supplement to the results from the simulations, we have analyzed the T_1 mapping data in the previous contrast agent uptake in vivo scans in order to establish the signal behavior during the mapping, as illustrated in Fig. 1. We have especially focused on voxels with high flow, since the

signal behavior is most likely to stand out from mono-exponential recovery in this case. This is because the contrast agent concentration gradient will be largest in those voxels. The scan parameters of the in vivo scans were similar to set-up A except that the number of alpha pulses was 10 instead of 12.

The in vivo examinations were performed with a specially implemented LL-EPI pulse sequence on a 1.5 T Signa scanner (General Electric Medical Systems, Milwaukee, WI, USA) with echo-planar imaging capacity. Omniscan (Nycomed, Oslo, Norway) was used as the gadodiamide contrast media.

4. Results

4.1. Simulations

Fig. 3 shows $1/T_{1,\text{error}}$ ($= 1/T_1 - 1/T_{1,\text{ideal}}$) versus the rate of change of the contrast concentration of the in-flowing tissue. The $1/T_1$ values were calculated using Eq. (1) and Eq. (2) with the correct α and τ , and χ adjusted to make $1/T_1$ and $1/T_{1,\text{ideal}}$ coincide under model supported conditions, i.e. in the origin of the plots. In this figure the inflow quantity was set to resemble a large vessel voxel (10 voxel volumes per second). Fig. 4 shows the result from the simulations when the inflow in the voxel was set to match the perfusion in normal perfused tissue (0.01 voxel volumes per second).

The results from the simulated vessel voxel in combination with scan parameter set-ups A–C show that for the low starting contrast concentrations (0.0 and 0.1 mM) $1/T_{1,\text{error}}$ is within 0.5 s^{-1} for concentration changes up to 1 mM s^{-1} . In general, for set-ups A–C concerning all starting contrast agent concentrations (0.0, 0.1, 0.5 and 1.0 mM), the in-flowing tissue cannot change more rapidly than 0.2 mM s^{-1} if the error tolerance criterion is to be held. Set-up D is noticeably less accurate than the other three set-ups and the results from set-ups A and C are very similar. In general, set-up B is the most accurate.

In the simulated tissue voxel, the results show that the error in $1/T_1$ is less than 0.1 s^{-1} for all simulated set-ups and concentration changes up to 1 mM s^{-1} , except set-up D in some special situations. In general, set-up D is clearly a less accurate set-up and set-up B the most accurate. Moreover, the error level is exceeded more easily if the starting contrast concentration of the voxel is high (diamonds in the plots) than when the concentration is low (circles). This is true for all the set-ups in both the simulated vessel voxel and in the simulated tissue voxel.

4.2. In vivo

Fig. 5 shows signal behaviors during a mapping of a single voxel VOI in the sagittal sinus from an in vivo examination. Fig. 5A shows the MRI signal behavior of the

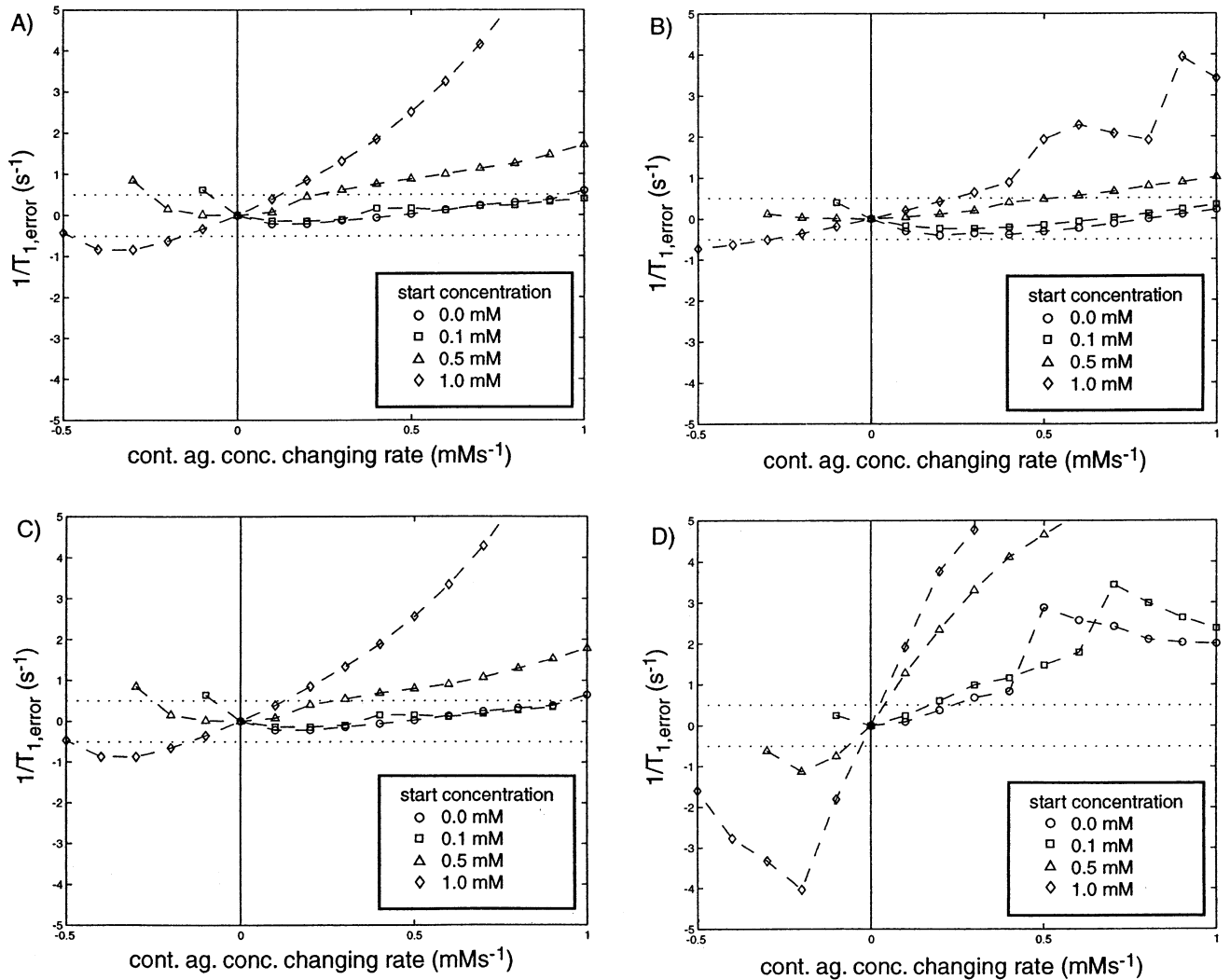


Fig. 3. This figure shows how $1/T_{1,error}$ varies in a typical vessel voxel when the contrast concentration of the in-flowing tissue changes linearly during the mapping. The four curves (marked with circles, squares, triangles and diamonds) show the simulation result for the different starting contrast concentrations 0, 0.1, 0.5 and 1 mM in the voxel. The dotted lines indicate an error tolerance level of 0.5 s^{-1} .

VOI prior to the contrast agent injection, and Fig. 5B the data from a mapping several minutes after the injection when the contrast agent concentration in the blood is stable. These two subplots show situations when the model holds. Fig. 5C–D shows the signal during mappings about 30 and 50 s respectively after the start of the normal dose injection (a 25 s long injection at 0.5 mL s^{-1}). These two mappings are at points in time when the contrast agent concentration gradient in the blood is large. These two subplots show situations in which the model cannot reproduce the MRI signal behavior during the mapping.

5. Discussion

The results from all the simulations of the normal perfused tissue indicate that only a small error is committed by fitting the data to Eq. (1). This is true for all simulated

non-supported situations except that in which the signal is highly dependent on the transversal relaxation rate (set-up D) and the contrast concentration of the in-flowing tissue is decreasing fast during the mapping. The situation in which the contrast agent concentration of the in-flowing tissue is decreasing fast is an unlikely in vivo situation, although it could conceivably occur just after a bolus passage of contrast agent in well perfused tissue with a high extraction fraction. To summarize, the results do not indicate any problem in performing dynamic T_1 mapping in normal perfused tissue as concerns a changing contrast agent concentration in the in-flowing tissue during the mapping.

In the vessel voxel simulations, especially if the duration of the mapping is long or the signal is highly dependent on the transversal relaxation rate, the results point to problem even when the absolute contrast concentration gradient of the in-flowing tissue is relatively small. For this reason, the

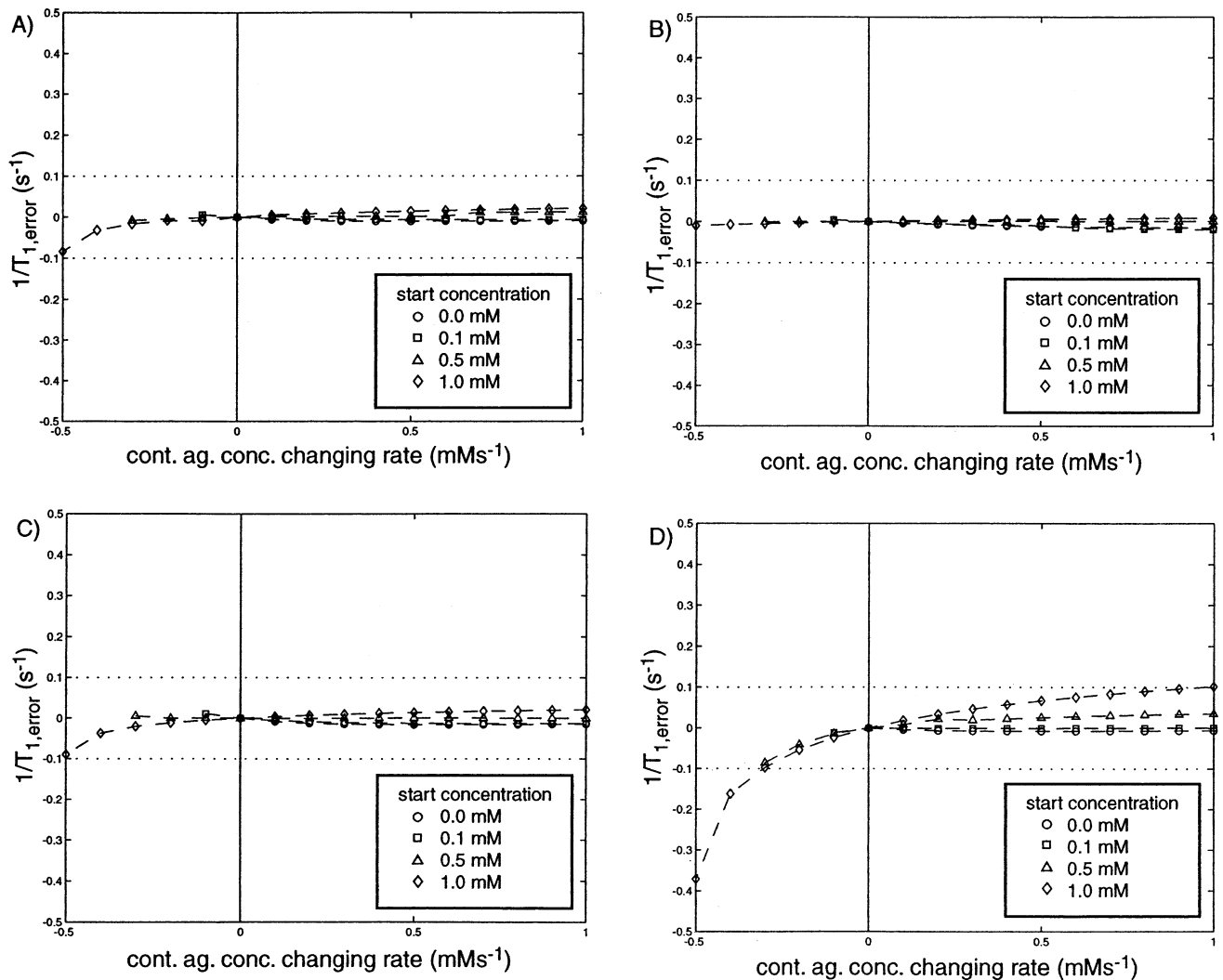


Fig. 4. This figure shows how $1/T_{1,error}$ varies in a normal perfused tissue voxel when the contrast concentration of the in-flowing tissue changes linearly during the mapping. The four curves (marked with circles, squares, triangles and diamonds) show the simulation result for the different starting contrast concentrations 0, 0.1, 0.5 and 1 mM in the voxel. The dotted lines indicate an error tolerance level of $0.1 s^{-1}$.

possibility of a bolus injection of contrast media is excluded if the goal is to track the tracer concentration in the blood with the LL-EPI T_1 mapping method. Instead, to minimize this problem, a non-bolus injection is recommended. The in vivo data shows that an injection rate at $0.5 mL s^{-1}$ is too high. Roughly, we estimate that an injection rate higher than $0.2 mL s^{-1}$ is not to be recommended, but this remains to be validated.

Comparing the results from the vessel voxel simulations with set-ups A and D shows that the effect of the contrast agent on the T_2^* value has a great influence on the feasibility of calculating a correct $1/T_1$ or $1/T_{1,eff}$ value. It is therefore recommended that the lowest possible echo time should be used in order to minimize the effect of T_2^* on the signal. This is also recommended for other reasons, e.g. to maximize the MRI signal. In summary, the results from the vessel voxel simulations with set-ups A and B indicate that a short duration of the mapping is preferable for situations in which

the contrast concentration in the voxel changes rapidly. This is because the changing contrast concentration of the in-flowing tissue then has a shorter time to influence the contrast concentration in the voxel. Comparing the results from the vessel simulation with set-ups A and C testifies to the fact that the alpha pulse flip-angle has little or no influence on the feasibility of calculating a correct $1/T_1$ or $1/T_{1,eff}$ value.

It should be pointed out that only a limited number of simulated relaxation values have been studied in this work, but since most human tissues and tumor relaxation times are to be found within this range, these can be regarded as relatively general results. It must also be pointed out that only two different inflow quantities have been used in these simulations. In in vivo conditions, a wide spectrum of inflow quantities may occur, especially in vessels.

It is important to stress that these simulations were fo-

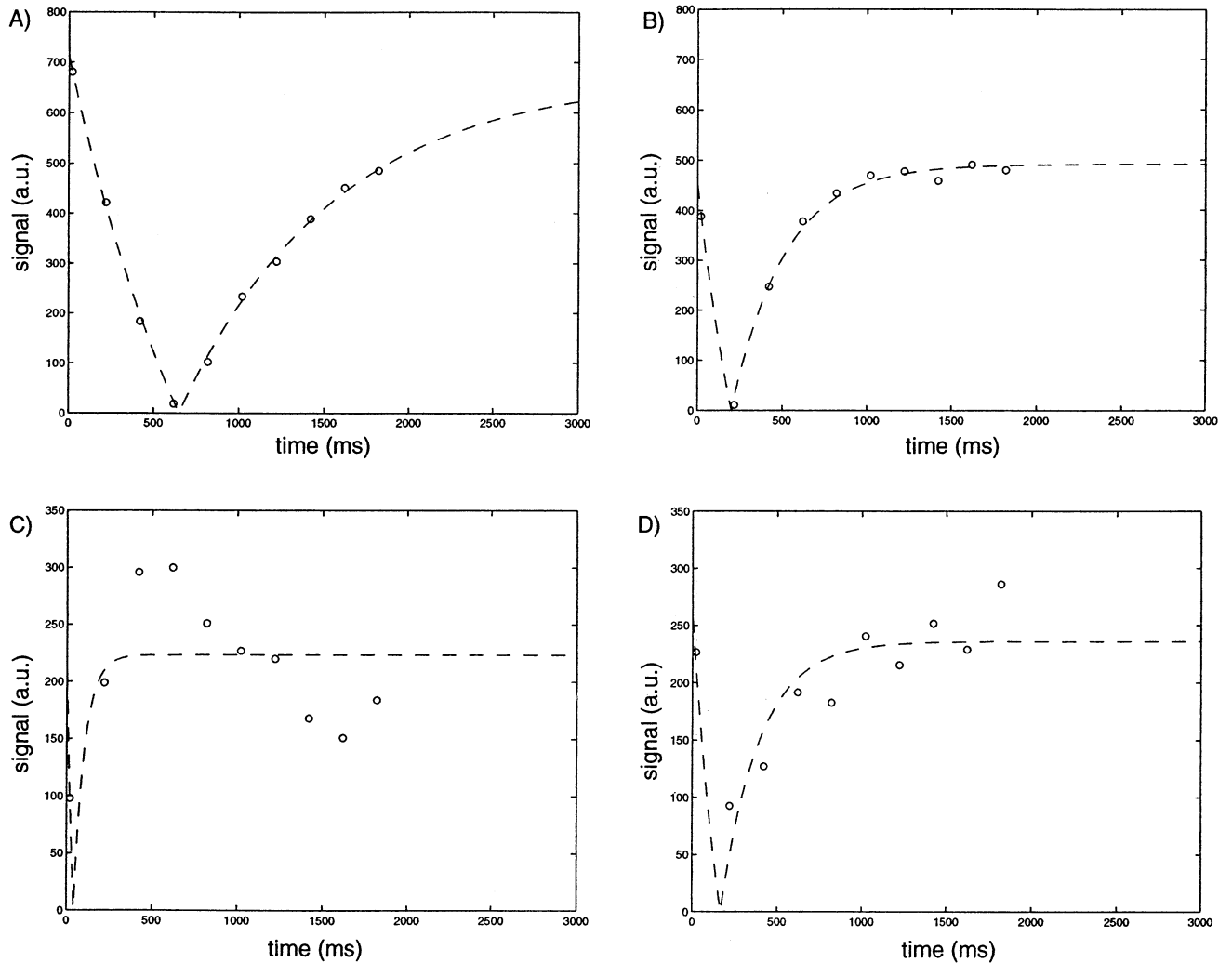


Fig. 5. In vivo (sagittal sinus) data of the MRI signal (circles) during LL-EPI T_1 mappings. The dashed lines are the least-squares fits (Eq. 1) of the data points A, a mapping prior to the contrast injection. B, a mapping several minutes after the injection. C, a mapping during a time when the contrast concentration is increasing considerably. D, a mapping during a time when the contrast agent concentration is decreasing appreciably in the blood.

cused on the feasibility of calculating a correct $1/T_1$ or $1/T_{1,\text{eff}}$ value for situations in which the longitudinal and transversal relaxation rates change during the mapping. No consideration was paid to noise and scan parameter optimization. Optimization of scan parameters (α , τ and n) has previously been performed [9,10,14]. These simulations nevertheless give an indication of the limits of the LL-EPI T_1 mapping technique, as can also be seen in the in vivo mapping data.

The in vivo data show that mapping behaviors occur in vivo, as has been shown in the simulations. We have found several MRI signal behaviors in our in vivo T_1 mapping data, as shown in Fig. 5C. All these behaviors are found in large vessels and at the time when the contrast concentration is increasing prominently in the blood, whereas behaviors as shown in Fig. 5D are more rare and they are found in vessels when the contrast concentration is decreasing in the blood.

6. Conclusion

This simulation indicates that the LL-EPI T_1 mapping method can be used in dynamic contrast uptake studies, but with some reservation. If only the paramagnetic contrast agent concentration of micro-vessel (capillary) tissue is of interest, any kind of injection, including a bolus, can be used. If, in addition to this, the contrast agent concentration of the blood in a large vessel is also of interest, e.g. for use as an input-function, a non-bolus injection must be used.

Acknowledgment

This study was partly supported by the Cancer Society in Stockholm (Grant 98:132).

References

- [1] Tofts SP, Brix G, Buckley DL, Evelhoch JL, Henderson E, Knopp MV, Larsson HBW, Lee TY, Mayr NA, Parker GJM, Ruediger EP,

- Taylor J, Weisskoff RM. Estimating kinetic parameters from dynamic contrast-enhanced T_1 -weighted MRI of a diffusable tracer: standardized quantities and symbols. *J Magn Reson Imaging* 1999; 10:223–32.
- [2] Su MY, Jao JC, Nalcioglu O. Measurement of vascular volume fraction and blood-tissue permeability constants with a pharmacokinetic model: studies in rat muscle tumors with dynamic Gd-DTPA enhanced MRI. *Magn Reson Med* 1994;32:714–24.
- [3] Verstraete KL, Van der Woude HJ, Hogendoorn PCW, De Deene Y, Kunnen M, Bloem JL. Dynamic contrast enhanced MR imaging of musculoskeletal tumors: basic principles and clinical applications. *J Magn Reson Imaging* 1996;6:311–21.
- [4] Griebel J, Mayr NA, De Vries A, Knopp MV, Gneiting T, Kremser C, Essing M, Hawighorst H, Lukas PH, Yuh WTC. Assessment of tumor microcirculation: a new role of dynamic contrast MR imaging. *J Magn Reson Imaging* 1997;7:111–9.
- [5] Larsson HBW, Fritz-Hansen T, Rostrup E, Søndergaard L, Ring P, Henriksen O. Myocardial perfusion modeling using MRI. *Magn Reson Med* 1996;35:716–26.
- [6] Zheng J, Venketesan R, Haacke EM, Cavagna FM, Finn PJ, Li D. Accuracy of T_1 measurements at high temporal resolution: feasibility of dynamic measurement of blood T_1 after contrast administration. *J Magn Reson Imaging* 1999;10:576–81.
- [7] Look DC, Locker DR. Time saving in measurement of NMR and EPR relaxation times. *Rev Sci Instrum* 1970;41:250–1.
- [8] Mansfield P. Multi-planar image formation using NMR spin echoes. *J Phys C* 1977;10:L55–L58.
- [9] Gowland P, Mansfield P. Accurate measurement of T_1 in vivo in less than 3 seconds using echo-planar imaging. *Magn Reson Med* 1993;30: 351–4.
- [10] Freeman AJ, Gowland P, Mansfield P. Optimization of the ultrafast Look-Locker Echo-Planar imaging T_1 mapping sequence. *Magn Res Imaging* 1998;16:765–72.
- [11] Alsaadi BM. Hydration of complexone complexes of lanthanide cations. *J Chem Soc* 1980;2151–4.
- [12] Weinmann HJ, Brasch RC, Press WR, Wesbey GE. Characteristics of gadolinium-DTPA complex: a potential NMR contrast agent. *Am J Roentgenol* 1984;142:619–24.
- [13] Strich G. Tissue distribution and magnetic resonance spin lattice relaxation effects of gadolinium-DTPA. *Radiol* 1985;154:723–6.
- [14] Karlsson M, Nordell B. Phantom and in vivo study of the Look-Locker T_1 mapping method. *Magn Res Imaging* 1999;17:1481–8.
- [15] Marquardt DW. An algorithm for least-squares estimation of nonlinear parameters. *J Soc Ind Appl Math* 1963;11:431–41.
- [16] Donahue KM, Weisskoff RM, Burstein D. Water diffusion and exchange as they influence contrast enhancement. *J Magn Reson Imaging* 1997;7:102–10.